WP15ER-PR(17) 18428

M Cipriani et al.

Laser-supported hydrothermal wave in low-dense porous substance

Preprint of Paper to be submitted for publication in
Laser and Particle Beams

This work has been carried out within the framework of the EUROfusion Consortium and has received funding from the Euratom research and training programme 2014-2018 under grant agreement No 633053. The views and opinions expressed herein do not necessarily reflect those of the European Commission.

Laser-supported hydrothermal wave in low-dense porous substance

M. Cipriani[1], S.Yu. Gus'kov[2,3], R. De Angelis[1], F. Consoli[1], A.A. Rupasov[2], P. Andreoli[1], G. Cristofari[1], G. Di Giorgio[1], F. Ingenito[1]

[1] *ENEA, Fusion and Technologies for Nuclear Safety Department, C.R.Frascati, via E. Fermi 45, 00044 Frascati (Rome,) Italy*
[2]*Lebedev Physical Institute, Leninskii Prospect 53, Moscow 119991, Russian Federation*
[3]*National Research Nuclear University MEPhI (Moscow Engineering Physics Institute), Kashirskoe av. 36, Moscow 115409, Russian Federation*

Abstract

The generalized theory of terawatt laser pulse interaction with low-dense porous substance of light chemical elements in a wide region of parameter variation is discussed. The theoretical model of laser-supported hydrothermal wave in a partially homogenized plasma of such a substance, including laser light absorption and energy transfer, is described. Laser light absorption, hydrodynamic motion and electron thermal conductivity are implemented in the hydrodynamic code, according to the degree of laser-driven homogenization of the laser-produced plasma. The results of numerical simulations obtained by using the hydrodynamic code are presented. The features of laser-supported hydrothermal wave in both possible cases of a porous substance with a density smaller and larger than critical plasma density are discussed along with the comparison with the experiments. The results are addressed to the development of design of laser thermonuclear target and powerful neutron and X-ray sources.

1. Introduction

Over the past 20 years, various laboratories have been actively studying the interaction of a nanosecond laser pulse of terawatt power with a substance that has an internal stochastic or regular structure in the form of solid elements, typically membranes or filaments, separated by vacuum gaps. The purpose of these studies is to obtain new knowledge about the fundamental processes of formation of high-temperature non-stationary laser-produced plasma and to develop important applications in the fields of laser thermonuclear fusion (LTF) and powerful sources of ionizing radiation. The discussed materials with stochastic structure are foams of light chemical elements, the most known of which are porous plastics ($[CH]_n$, $[CH_2]_n$), agar-agar ($C_{12}H_{18}O_9$), threeatsetat-cellulosa (TAC, $C_{12}H_{16}O_8$), trimethylolpropane triacrylate (TMPTA, $C_{15}H_{20}O_6$) and polyvinylalcohol (PVA, $[CH_2CH(OH)]_n$). The average density of porous media can vary over a wide range,

from several mg/cm^3 to several hundred mg/cm^3. Thus, according to specific experimental needs, it is possible to select porous media with an average density either larger or smaller than the critical plasma density corresponding to laser wavelengths from several microns up to a few tens of a micron. The pore sizes can vary from a few microns to several tens of microns when the thickness of solid elements varies from several hundreds of a micron to several microns.

Due to its low density and heterogeneous structure, such a substance can be used as the constituent of a direct-driven LTF target for effective volume absorption of the laser radiation (Gus'kov, 1995; Gus'kov, 1997a; Bugrov, 1997; Gus'kov, 2000a), providing a high absorption efficiency exceeding 80% for a Nd-laser radiation, as registered in experiments (Bugrov, 1997; Gus'kov, 2000a; Bugrov, 1999; Caruso, 2000). Moreover, it can be employed to smooth the inhomogeneities in the distribution of absorbed laser energy (Gus'kov, 1995; Gus'kov, 1997a; Bugrov, 1997; Gus'kov, 2000a; Koch 1995; Desselberger, 1995; Dunne, 1995; Kalantar, 1997; Watt, 1997; Watt, 1998; Batani, 2000; Nishimura, 2000; Hall, 2002; Gus'kov, 2000b) and also to increase the degree of conversion of laser radiation into X-ray in the holhraum, in the context of indirect target drive scheme (Amendt, 2015). The doping of a porous material with heavy chemical elements can improve the conversion of laser radiation into X-rays. This feature can be relevant for a scheme of direct target irradiation by X-rays without the use of the holhraum (Gus'kov, 2001) as well as for the development of effective radiography methods (Fournier, 2010; Perez, 2014). Powerful laser sources of neutron and X-ray radiation can be realized (Gus'kov, 1997b) by using media constituted by a regular set of thin continuous solid layers or layers with holes located at a given angle to each other and separated by vacuum gaps, or by a set of spherical or cylindrical micro shells bordering each other.

In the first numerical simulations of the laser interaction with a volume structured substance the foam was modeled as a series of equally spaced parallel solid layers separated by vacuum gaps (Caruso, 1997). These results, as well as the similar ones obtained in (Kapin, 2006) with the same approach, showed a limitation of energy

transfer wave velocity both in the case of overcritical and subcritical foams. A more refined modeling was done in Gus'kov, (2000b) where the solid layers had circular cuts. The absorption coefficient resulted to be considerably larger than in the case of a homogeneous substance of the same average density. However, such an approach, which is adequate for regular structure, can give an incomplete and largely qualitative picture of phenomena in the case of porous target. A different approach for simulation consists in modeling the porous substance as a continuous medium with fixed specific properties for laser light absorption and energy transfer (Gus'kov, 2003; Lebo, 2009; Rozanov, 2016). This approach allows to obtain integral characteristics of energy transfer for a given type of porous substance and given experimental conditions, but the target properties do not evolve during the calculation. More recently, simulations have been performed with the two-dimensional hydrodynamic code PALE (Velechovsky, 2016), by implementing a two-scale model for laser light absorption and limiting electron conductivity depending on the homogenization degree of the plasma. Despite the quantitative agreement with the data of all known experiments with subcritical foams where ionization wave velocity was measured (Limpouch, 2004; Depierreux, 2009; Nikolai, 2012; Khalenov, 2006; Borisenko, 2006), the code is limited to simulate only subcritical foams with a closed pore structure.

In Gus'kov (2015) we developed an effective modeling of the foam absorption properties. In this model the absorption efficiency in the foam target depends on the degree of homogenization of the plasma. As a consequence, the foam characteristics vary in space and time according to the state of the plasma. Moreover, this model can be applied to overcritical and subcritical porous media, with small and large pores. The main assumption of the model is that laser radiation is absorbed via the inverse bremsstrahlung process while it propagates in the stochastically distributed regions of plasma with subcritical density, formed during the collision of expanding matter of the heated solid elements. In the calculations in Gus'kov (2015), the ionization wave in a subcritical substance resulted to be 2 times slower than the self-similar solution

(Denavit, 1971) for a homogeneous substance of the same density, in accordance with the experiments. This work is the further development of this approach. The absorption model has been implemented in a hydrodynamic code, with the addition of limitations on electron thermal conductivity and hydrodynamics, the former due to the partial lack of free electrons in the filling pores, the latter to the inhomogeneity of the plasma density. A new one-dimensional hydrodynamic code describing the interaction of laser radiation with a porous substance of the various types has been developed and named MULTI-FM, which is a modification of the well-known MULTI code (Ramis, 1988) with the inclusion of macroscopic models of absorption of laser radiation and energy transfer in porous media. The description of this code and the discussion of the simulations made with it are the main topics of this work, which is intended to be a reference for the research on porous media, discussing the principal features of the plasma created by high power laser.

The paper is organized as follows. The second section describes the main features of the theoretical model at the basis of the code. The third section describes the MULTI-FM code and the results of simulations performed with this code modeling the formation and evolution of the laser-produced plasma in various foams. A comparison with numerical calculations and experimental data known from the literature is given in the fourth section. The last section is devoted to conclusion and discussion of future work on the subject.

2. Physical phenomena

The key mechanism that determines the features of laser interaction with porous matter and the properties of the resulting plasma in the model is the viscous homogenization in the heated region of matter (Gus'kov, 2000b). The structure of a porous substance is described with the help of a fractal parameter α in the form (Amendt, 2015)

$$\frac{\delta_0}{b_0} \approx \left(\frac{\rho_s}{\rho_p}\right)^{\alpha} \qquad (1)$$

where δ_0 and b_0 are, respectively, the average pore size and solid element thickness; ρ_s and ρ_p are, respectively, the initial density of solid elements and the average density of the foam.

The parameter α depends on the form of solid elements and is approximately equal to $(\nu+1)^{-1}$, where the values ν=0, 1, 2 correspond to its planar (membrane), cylindrical (filament) or spherical (cluster) form. For the membrane-filamentary structure mentioned in the introduction, which characterizes most of the light foams, the value α=0.8 provides the best agreement of theoretical estimates with the experimental data, especially for the homogenization rate (Gus'kov, 2011). The characteristic time of homogenization, which is determined by the ion-ion collision time, is

$$\tau_0 \approx 2.4\cdot 10^{-3}\frac{Z^4\left(\delta_0 - b_0\right)^2\rho_p}{A^{1/2}T^{5/2}} \approx 2.4\cdot 10^{-3}\frac{Z^4\delta_0^2\rho_p}{A^{1/2}T^{5/2}},\quad s \qquad (2)$$

where T is the plasma temperature and A and Z are the atomic weight and charge of plasma ions, respectively. The homogenization time is several tens of picoseconds for a small-pore substance and several nanoseconds for a large-pore substance, for laser intensity exceeding 10^{13} W/cm^2, heating the plasma to temperatures up to several hundreds of eV or more.

The absorption coefficient derived in (Gus'kov, 2015) is defined as the inverse value of the transparency length of a substance with a stochastic distribution of the regions of overcritical density, whose cross section increases as the homogenization process develops:

$$K_p(x,t) = \frac{\delta_0}{b_0 L_{p0}}\left\{\frac{1}{\left(1-\frac{b_0}{\delta_0}\right)\left[1-H\left(x,t\right)\right]^{1/2}} - 1\right\} \quad , 0 \le t \le t_h \qquad (3)$$

In this expression the initial transparency length is expressed as:

$$L_{p0} \approx \frac{\pi^2}{2} \frac{\rho_s}{\rho_p} b_0 \qquad (4)$$

and the function $H(x,t)$ characterizes the degree of homogenization increasing with time:

$$H\left(x,t\right) = 2\int_0^t \frac{dt'}{\tau_0\left(x,t'\right)}, \quad 0 \le H(x,t) \le H(x,t_h) \qquad (5)$$

At the homogenization time, the degree of homogenization is:

$$H(x,t_h) = H_c = \begin{cases} 1 & , \quad \rho_p \ge \rho_{cr} \\ 1 - \left[\dfrac{1 - \left(\dfrac{\rho_p}{\rho_{cr}} \right)^{\alpha}}{1 - \left(\dfrac{\rho_p}{\rho_s} \right)^{\alpha}} \right]^2 & , \quad \rho_p \le \rho_{cr}, \end{cases} \qquad (6)$$

These values are due to the different criterion for defining the plasma to be homogeneous in the two cases. In overcritical foams, the plasma is considered to be homogeneous when the degree of homogenization is equal to 1, meaning that there are no more spatial density variations and that the plasma is opaque to the laser light. In the case of subcritical foams, the plasma is homogeneous when the maximum of the spatial density variations is lower than the critical density, resulting in the value of the homogenization degree in (6).

Because of the partial lack of free electrons in the filling pores, the homogenization process affects the velocity of the ionization wave in the subcritical foam and the velocity of the electron conductivity wave in both subcritical and overcritical foams. In fact, the speed of both these energy transfer processes is limited by the speed of propagation of the homogenization wave. Due to the explosive nature of the expansion of thin pore walls, the propagation velocity of the homogenization wave can slightly exceed the speed of sound in an equivalent homogeneous medium with the same average density; on the other hand, the scale of homogenization wave speed is the sound speed. As a result, the energy transfer wave velocity is

significantly lower than the ionization wave or the electron conductivity wave velocity in an equivalent subcritical or overcritical homogeneous medium (having the same average density), respectively. Measurements of the ionization wave velocity in the subcritical foams and the velocity of energy transfer wave in the overcritical foams, which prove the fact that these velocities were limited to the sound speed, were experimentally performed. The wave of energy transfer in a foam was named hydrothermal wave (Bugrov, 1997) and the temperature distribution behind its front is uniform due to rapid equalization by electron thermal conductivity. Behind the hydrothermal wave front, part of the energy is contained in the energy of stochastically colliding plasma flows, so that the degree of homogenization determines the magnitude of the pressure gradient and, as a consequence, the velocity of the mechanical wave. For this reason, it can be concluded that the hydrothermal wave in the early stage of homogenization is an acoustic or weak shock wave, and only at a considerable degree of homogenization it can be transformed into a strong shock wave with a sharp front of the compression region.

3. Numerical simulation results

Numerical simulations of this work are performed using the one-dimensional hydrodynamic code MULTI-FM where the models of absorption, motion, and electron thermal conductivity of a porous substance of arbitrary density are implemented.

In the MULTI-FM code, the degree of homogenization, governing all the relevant properties of the foam plasma, is determined in each numerical cell by the parameter

$$\mathrm{IsFoam}(x,t) = 1 - \frac{H(x,t)}{H_c} \tag{9}$$

in which $H(x,t)$ and H_c are determined by expressions (5) and (6). The parameter IsFoam is equal to 1 for the cells not yet reached by the laser (cold material) and continuously varies according to the homogenization degree of the cell down to the value 0, at which the plasma is completely homogeneous. To realize the expected smooth transition from foam-like to inverse bremsstrahlung absorption in the

inhomogeneous plasma, the total absorption coefficient is calculated, as a first approximation, by the formula:

$$K(x,t) = \sqrt{\left(K_f(x,t) \cdot \mathrm{IsFoam}(x,t)\right)^2 + \left(K_b(x,t) \cdot (1 - \mathrm{IsFoam}(x,t))\right)^2}, \quad (10)$$

where $K_f(x,t)$ is the absorption coefficient of Equation (10), while $K_b(x,t)$ is the inverse bremsstrahlung absorption coefficient. The IsFoam parameter is evaluated in the beginning of the calculation for the current time-step in the code, along with the absorption coefficient, using the values of the parameters from the previous time-step.

To reproduce the limitation of pressure action and electron conductivity we introduce the parameter $\eta(x,t) = 1 - \mathrm{IsFoam}(x,t)$ in the momentum and in the heat equations as:

$$\frac{\partial}{\partial t} v(x,t) = -\eta(x,t) \frac{\partial}{\partial m} P(x,t) \quad (11)$$

$$q(x,t) = -\eta(x,t) \left[\chi(x,t) \frac{\partial T_e(x,t)}{\partial x}\right] \quad (12)$$

where $v(x,t)$ is the velocity of the plasma, m is the Lagrangian mass coordinate and $P(x,t)$ is the pressure; $q(x,t)$ is the heat flux, $\chi(x,t)$ is the Spitzer conductivity and $T_e(x,t)$ is the electron temperature. This parameterization allows changing the energy transport and mechanical properties of the homogenizing plasma in accordance with its homogenization degree.

Subcritical and overcritical polystyrene foams with small and large pores have been simulated using the MULTI-FM code. The results of the simulations in the different regimes are reported and discussed in detail, in order to provide an in-depth analysis of the laser-produced plasma properties in foam materials. The solid parts density is of 1 mg/cm^3 and average density is equal to 10 mg/cm^3. The laser wavelength has been varied to change the critical density without changing the target density, namely from $\lambda_{\mathrm{over}} = 1054$ nm for overcritical foam cases to $\lambda_{\mathrm{sub}} = 351$ nm for subcritical foams. Note that all low-dense foams mentioned in introduction and used in recent experiments have a similar chemical composition and density of solid

elements. In the simulations of the following section the laser intensity has been chosen as $I_L=10^{14}$ W/cm^2 and the value of the fractal parameter was chosen to be α = 4/5, corresponding to the typical membrane-filamentary structured foams used in the recent experiments. The target is taken very thick, namely 2 mm for large-pore foams and 200 μm for small-pore foams, in order to have room for all the thermal and hydrodynamic waves to develop completely in the time of the simulation. All results are compared with calculations of a homogeneous substance with the same average density, in order to highlight the peculiar differences between the two cases. We initially present the results of simulations where hydrodynamics and electron thermal conductivity are initially switched on separately, to decouple their effect on the homogenization wave. Such calculations are shown only for larger-pore overcritical foam, where the effect is more evident.

3.1 Large-pore foams of overcritical density

In the simulations with a large-pore foam target as the ones in this and in the following subsection, the pore size is taken $\delta_0 = 40$ μm, corresponding to a solid part thickness b_0=1 μm (see, (1)). The initial geometric transparency length results to be L_0=492 μm (see, (4)). The conditions of simulations correspond to the experiments on Nd-laser of the ABC installation of the ENEA Frascati Research Center (De Angelis, 2015; Cipriani, in preparation).

3.1.1 Heat conduction without hydrodynamics

The curves of Fig. 1 are taken at different times in the simulation. The dynamics of the heat conduction wave is different before and after the time instant t_h = 1.62 ns, which corresponds to the homogenization of the region heated by the laser radiation. At the beginning of the laser irradiation the foam absorbs the laser energy on a depth equal to the opacity length, while the homogeneous medium absorbs it at the front of the target. The time required for the foam plasma to become homogeneous delays the formation of the heat wave in panel (a) compared to panel (b). The temperature profile in panel (a) indicates that the heat wave is evident only when the plasma is

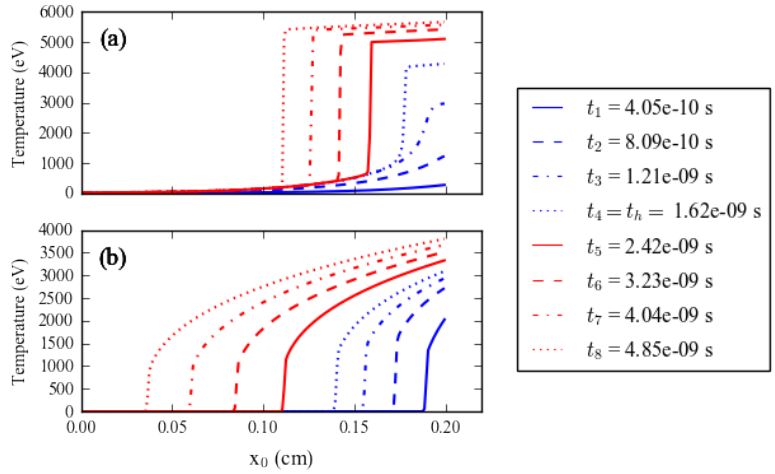

Figure 1. The temperature profiles in the simulation of a large-pore overcritical foam with the parameters described in the text. The hydrodynamics is suppressed. Panel (a) represents the temperature for a foam target; panels (b) represents the temperature for a homogeneous target with the same density as the foam one. The curves are taken at the different times of the simulation reported in the legend. The laser is coming from the right. In all panels, the horizontal axis corresponds to the position of the numerical cells at the initial time t_0.

almost homogeneous, for example at times t_3 or t_h, while in the homogeneous medium it is identifiable already at t_1. Ahead of the temperature front, the laser-produced foam plasma has formed but it is not homogeneous and the heat conduction is limited proportionally to the degree of homogenization; behind it the homogenization process has been completed and the heat conduction is fully operational. After the homogenization time the temperature profiles in panels (a) and (b) shows that the heat wave propagates into the target, at a higher speed in the homogeneous medium than in the foam: the speed of the thermal wave is $3.3\text{x}10^7$ cm/s in the homogeneous medium, while it is $2.2\text{x}10^7$ cm/s in the foam, with a ratio of 1.5. Thus, limiting the electron conductivity in large pore foams has a very important effect on the speed of the ionization wave.

3.1.2 Hydrodynamics without heat conduction

Comparing panels (a1) and (a2) of Fig.2 we can see that the delay in the laser absorption due to homogenization is found also in the formation of hydrodynamic wave in the foam. In panel (a2) the shockwave appears already at the initial time, while in the foam it is visible only at homogenization time t_h=1.52 ns. The compression wave appears later in the foam than in the ordinary homogeneous material. The wave is slightly slower in the foam than in the homogeneous medium.

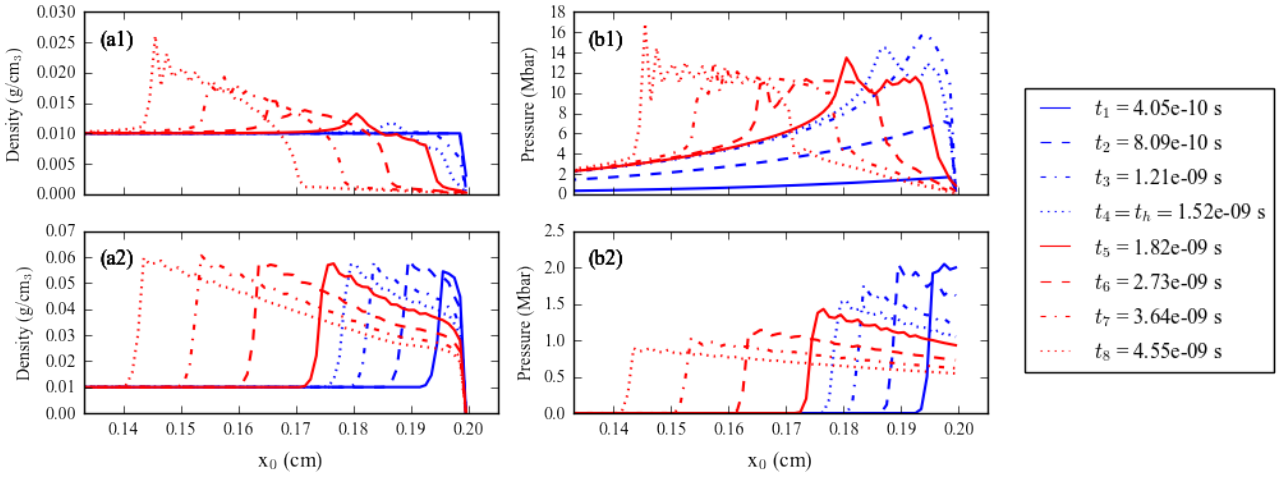

Figure 2. The density profiles in the simulation of a large-pore overcritical foam with the parameters described in the text. The heat conduction is suppressed. Panel (a1) and (b1) represent the density and the pressure for a foam target; panels (a2) and (b2) represent the density and the pressure for a homogeneous target with the same density as the foam one. The curves are taken at the different times of the simulation reported in the legend. The laser is coming from the right. In all panels, the horizontal axis corresponds to the position of the numerical cells at the initial time t_0.

At the beginning, the pressure is about one order of magnitude less in the foam in panel (b1) than in the homogeneous medium in panel (b2), due to the fact that before homogenization all the absorbed energy remained as internal energy of density oscillations. For times later than the homogenization time, the peak density in the foam (panel (a1) of Fig. 2) of 0.025 g/cm^3 is significantly less than the peak density of 0.06 g/cm^3 in homogeneous medium (panel (a2) of Fig.2). The position of the front of the compression wave is almost coincident in the two cases from the homogenization time on. This shows that the modification of Eq. (11) leads to physically correct results, which result in no delay of the compression wave propagation in the porous target, as well as lower peak of the density and larger peak of the pressure at the wave front in comparison with homogeneous medium.

3.1.3 Complete simulation

Figure 3 reports the simulation results with all the physical processes active. The features found in the previous subsections are all apparent. The density profile in (a1) shows that the hydrothermal wave in the foam develops later than in the homogeneous medium, in panel (a2). Also the panel (b1) shows the effect of electron conductivity suppression, giving a sharp front of the heat wave and a slow down of its propagation speed, compared to the homogeneous medium in (b2). The peak value

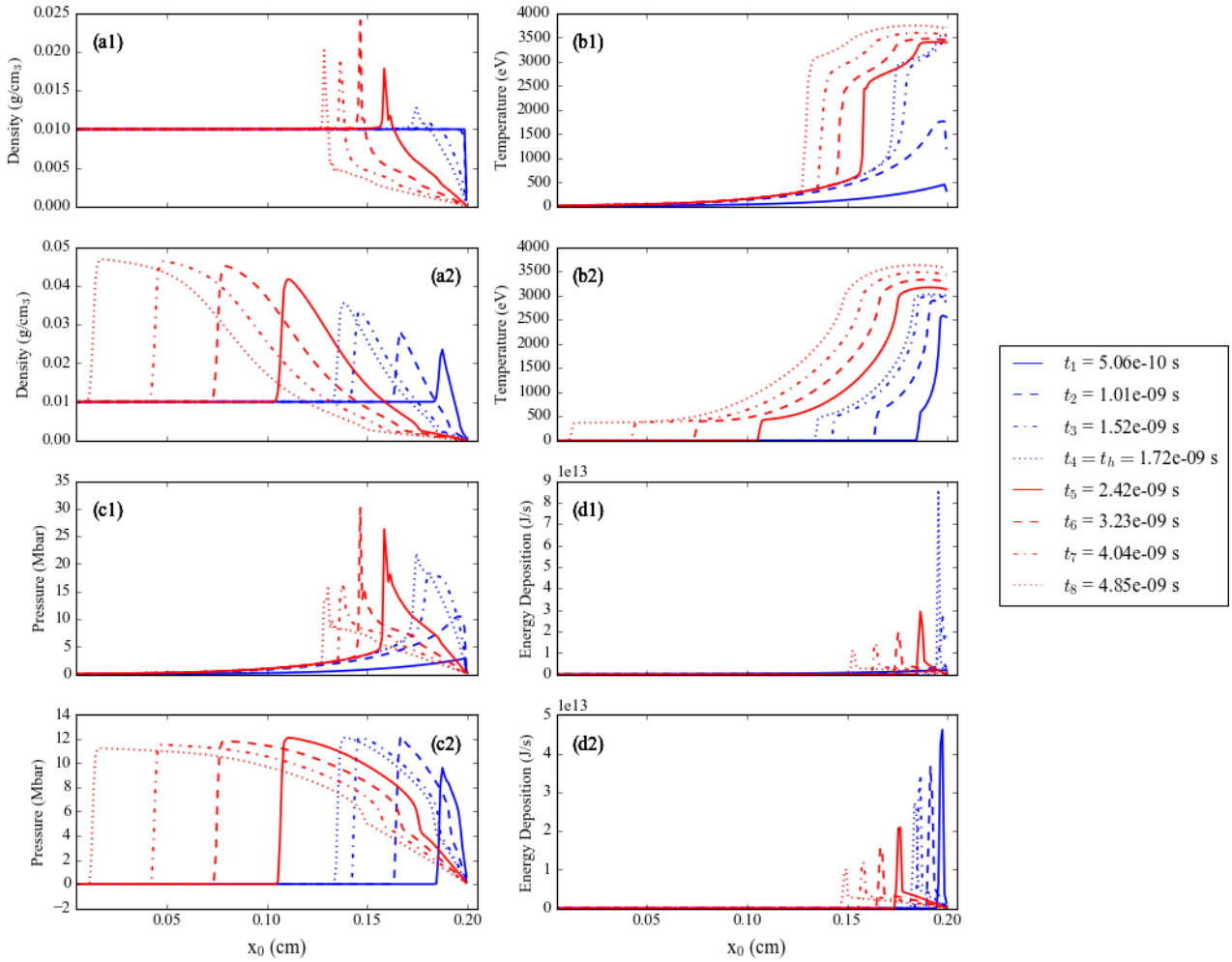

Figure 3. The profiles of the different physical quantities in the simulation of a large-pore overcritical foam with the parameters described in the text. Panels (a1), (b1), (c1), (d1) represent density, temperature, pressure and laser energy deposition respectively for a foam target; panels (a2), (b2), (c2), (d2) represent density, temperature, pressure and laser energy deposition respectively for a homogeneous target with the same density as the foam one. The curves are taken at the different times of the simulation reported in the legend. The laser is coming from the right. In all panels the horizontal axis corresponds to the position of the numerical cells at the initial time t_0.

of the pressure in (c1) can be estimated to be around 30 Mbar, and it is higher than the value of 12 Mbar in (c2). For times later than the homogenization time t_h=1.72 ns we can see from panels (a1) and (a2) that the hydrothermal wave moves into the target with a very different speed, as does the heat wave. The speed of the hydrothermal wave in the foam is $1.3 \cdot 10^7$ cm/s, that is less by factor 2.6 than the shock wave speed in the homogeneous medium ($3.4 \cdot 10^7$ cm/s). This shows that the low conductivity of the non-homogeneous foam plasma deeply affects the propagation speeds of these two waves. We conclude this section by stressing that the absorption mechanism in overcritical foams delays the formation of the compression wave and also defines the region of the laser-produced plasma where the heat

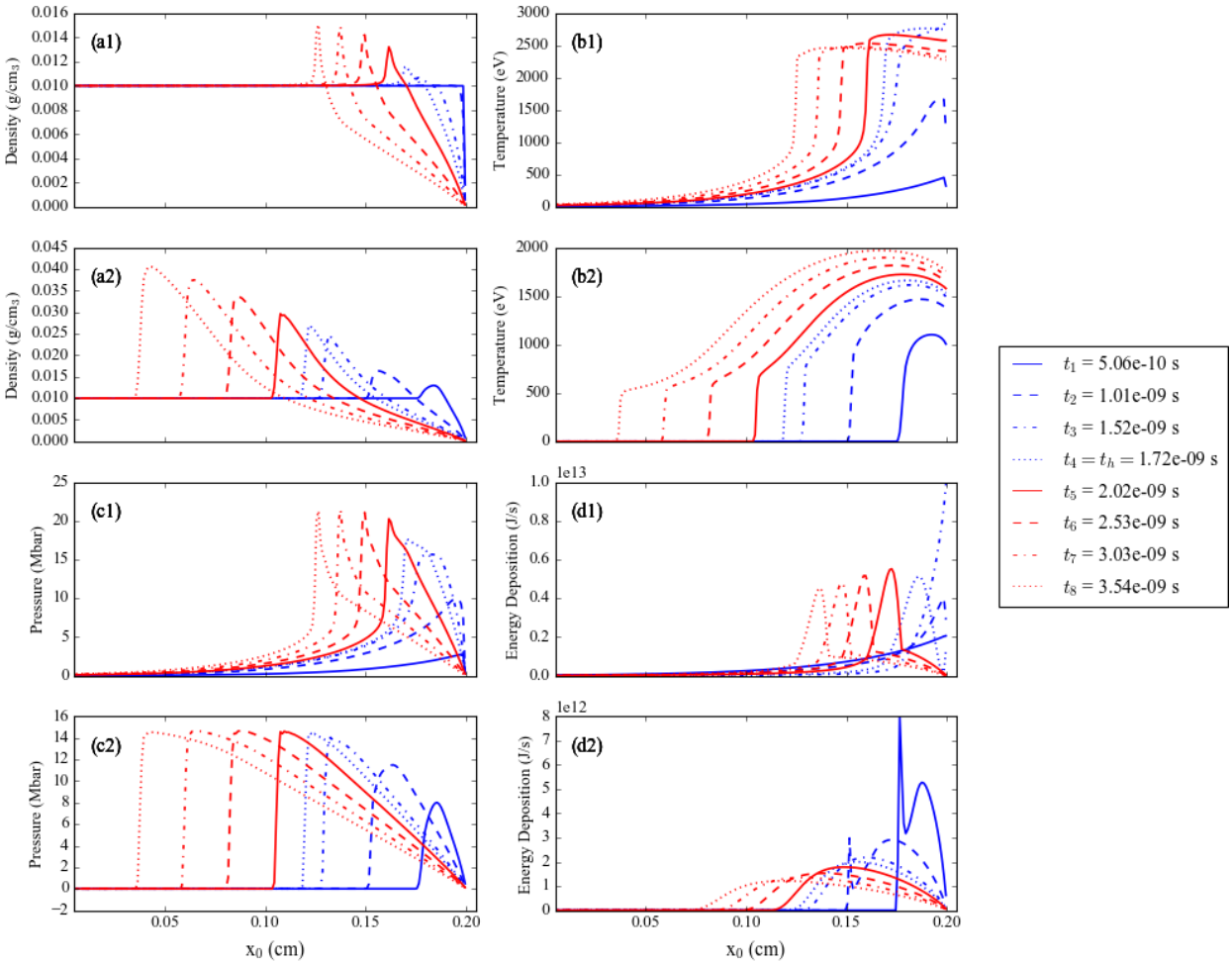

Figure 4. The profiles of the different physical quantities in the simulation of a large-pore subcritical foam with the parameters described in the text. Panels (a1), (b1), (c1), (d1) represent density, temperature, pressure and laser energy deposition respectively for a foam target; panels (a2), (b2), (c2), (d2) represent density, temperature, pressure and laser energy deposition respectively for a homogeneous target with the same density as the foam one. The curves are taken at the different times of the simulation reported in the legend. The laser is coming from the right. In all panels the horizontal axis corresponds to the position of the numerical cells at the initial time t_0.

conduction is effective. The heat conduction suppression is crucial to reproduce the slowdown of the ionization wave observed in the experiments.

3.2 Large-pore foams of subcritical density

The foam parameters δ_0 and b_0 are the same of the previous subsection, while the laser wavelength has been changed. The results of the complete simulation are reported in Fig. 4. As before, the formation of the compression wave is delayed in the foam up to around the homogenization time t_h=1.72 ns as seen in panel (a1), while in the homogeneous medium it appears already at time t_1, panel (a2). The speed of the hydrothermal wave in the foam is about $1.8 \cdot 10^7$ cm/s, that is less than the speed of shock wave in homogeneous medium by factor 2.5 ($4.5 \cdot 10^7$ cm/s). We also note that

the electron conductivity suppression slows down the heat wave as seen from the comparison between panels (b1) and (b2). The temperature at the front of the target reaches 2.5 keV in the foam in panel (b1), while in the homogeneous medium it is 2 keV. Moreover, the peak value of the pressure is higher in the foam in panel (c1) than in the homogeneous medium in panel (c2). The ratio of 1.4 between the former and the latter is lower than the ratio in the overcritical case, which results to be 1.8. Finally, the profiles of the energy deposited by the laser in panel (c1) clearly show the homogenization stage in the foam, going up to time t_h. During this period, the laser energy is absorbed in a layer up to a depth equal to the transparency length. Oppositely to the overcritical case, the end of the homogenization phase is smooth because the homogenized plasma absorbs the energy in a thick layer of the order of the inverse of the collision absorption coefficient, being the average density of the foam smaller than the plasma critical density.

3.3 Small-pore foams of overcritical density

For small-pore foams in this and in the following subsection, the pore size is $\delta_0 = 1$ μm, giving a solid part thickness b_0=0.025 μm. The initial transparency length L_0=12.3 μm correspond to these conditions. The plots of results are collected in Figure 5. The homogenization time is t_h=87 ps, that is 20 times smaller than in large-pore foam. This result correlates with estimation of characteristic time of homogenization τ_0, when, according (2), $\tau_0 \propto \delta_0^2/T^{5/2}$. For small-pore foam the pore size is 40 times less than for large-pore one. However, due to significantly faster hydrothermal wave, a larger mass of small-pore foam is heated and 3 times smaller plasma temperature is realized (at the same laser intensity) in comparison with large-pore foam case (see, figs 3, 4, 5). So, the estimation shows the more than one order less homogenization time in the case of small-pore foam in comparison with large-pore one. We also notice the features of the hydrothermal wave. The formation of the compression wave is delayed in the foam and it is barely distinguishable in the density plot in panel (a1), while in the homogeneous medium in panel (a2) it is evident already at time t_1. The hydrothermal wave speed in the foam is $1.8 \cdot 10^7$ cm/s ,

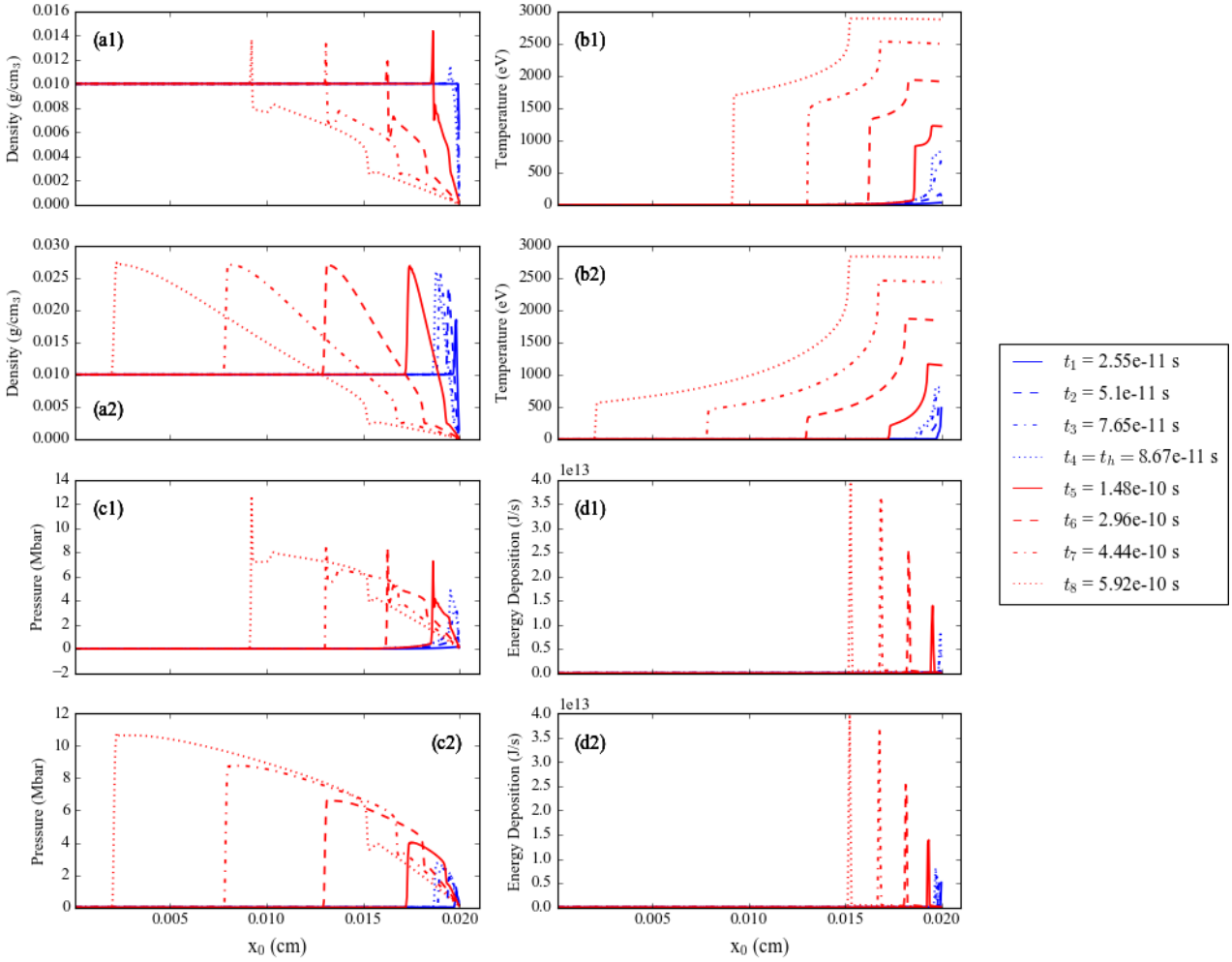

Figure 5. The profiles of the different physical quantities in the simulation of a small-pore overcritical foam with the parameters described in the text. Panels (a1), (b1), (c1), (d1) represent density, temperature, pressure and laser energy deposition respectively for a foam target; panels (a2), (b2), (c2), (d2) represent density, temperature, pressure and laser energy deposition respectively for a homogeneous target with the same density as the foam one. The curves are taken at the different times of the simulation reported in the legend. The laser is coming from the right. In all panels the horizontal axis corresponds to the position of the numerical cells at the initial time t_0.

that is 1.9 lower than the speed of the shock wave in homogeneous media ($3.4 \cdot 10^7$ cm/s, the same as shock wave speed in section 3.1.3) . Due to the small optical depth of the considered small-pore foam, the temporal dynamics of hydrothermal wave and the spatial distribution of deposited energy behind its front are closer to the case of homogeneous substance in comparison with large-pore case. In fact, in large-pore foams the homogenization process requires a longer time to be completed, and this results in an effective slow-down of the hydrothermal wave. Heat conductivity and response to pressure gradients are limited during the homogenization stage and thus the propagation speed of the heat and compression waves is reduced. In small-pore foams the homogenization time is very small and the limiting on the heat conduction

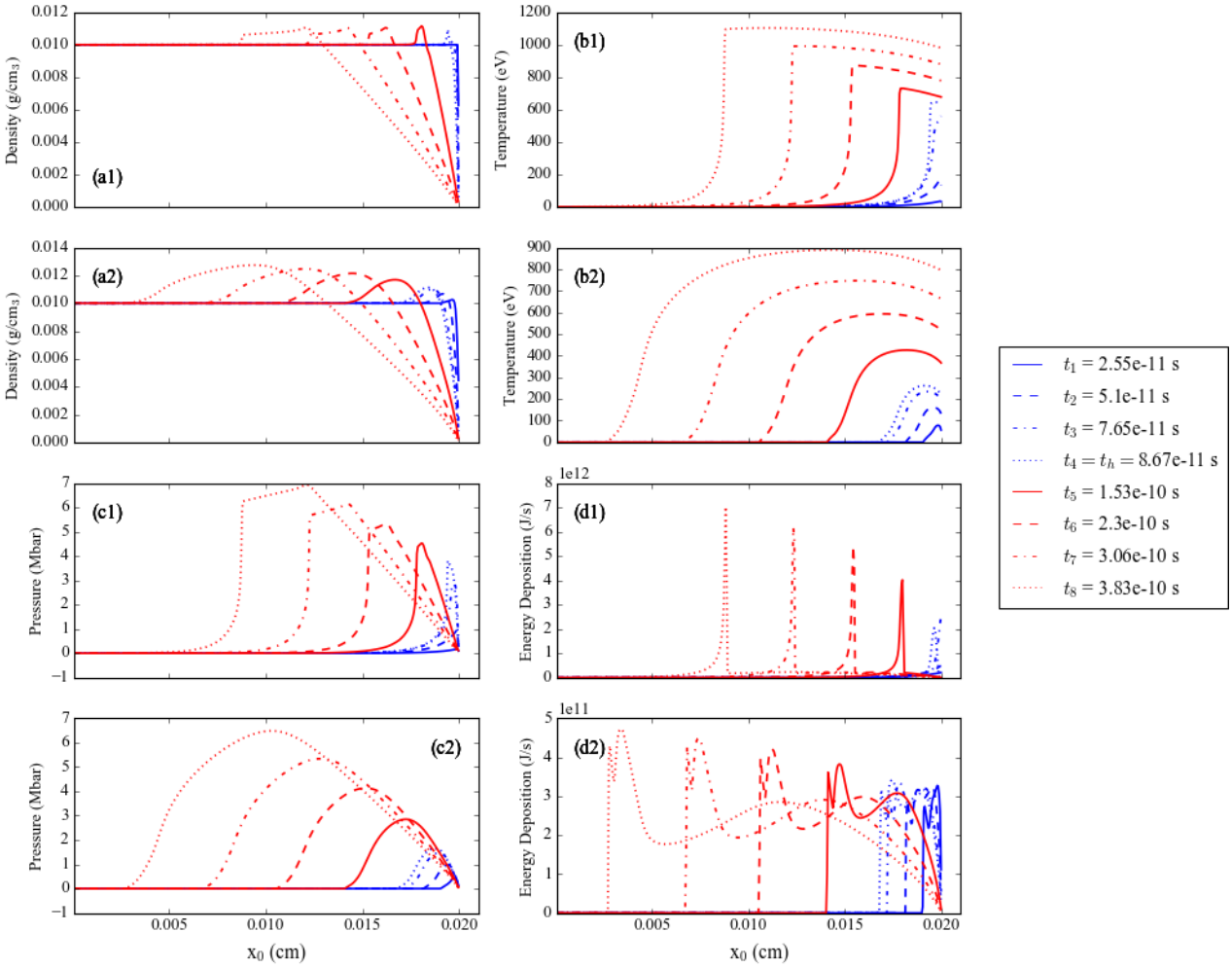

Figure 6. The profiles of the different physical quantities in the simulation of a small-pore subcritical foam with the parameters described in the text. Panels (a1), (b1), (c1), (d1) represent density, temperature, pressure and laser energy deposition respectively for a foam target; panels (a2), (b2), (c2), (d2) represent density, temperature, pressure and laser energy deposition respectively for a homogeneous target with the same density as the foam one. The curves are taken at the different times of the simulation reported in the legend. The laser is coming from the right. In all panels the horizontal axis corresponds to the position of the numerical cells at the initial time t_0.

and pressure is confined to a thin layer. Therefore, the hydrothermal wave speed in this last case is also reduced, but the slow-down is less effective than in large-pore foams. The peak pressure is higher in large-pore foams in Fig. 3(c1) than in small-pore ones in Fig. 5(c1).

3.4 Small-pore foams of subcritical density

The conditions of the simulation are the same of the previous subsection, with the shorter laser wavelength. The initial transparency length in this case is L_0=12.3 μm. These conditions are similar to ones of the recent experiments at PALS, GEKKO and OMEGA nanosecond laser facilities. The results of the simulation with a subcritical foam target are reported in Fig. 6. Comparing panels (d1) and (d2) we see that the

laser energy in the foam is mostly deposited at the homogenization front, where the absorption coefficient in the foam plasma has the highest value. This is different from what happens in the homogeneous medium, where a part of the laser energy is absorbed in the plasma corona and the rest at the ionization wave front, where the plasma is cold and the inverse bremsstrahlung absorption coefficient has its peak value. An important fact is that in the homogeneous plasma the laser energy is deposited on a thick layer in the target and penetrates at a larger depth compared to what happens in the foam plasma. The speed of the hydrothermal wave in small-pore foam of subcritical density is about $2.9 \cdot 10^7$ cm/s that is 1.5 times lower than the speed of the ionization wave in the homogeneous medium of the same density ($4.5 \cdot 10^7$ cm/s, the same as shock wave speed in the section 3.2), as can be seen from the temperature and density profiles in panels (a1) and (a2), and (b1) and (b2) respectively.

3.5 Influence of laser intensity and foam density

Table 1 presents a summary of the results of the simulations presented above, together with the results of simulations performed to demonstrate the dependence of the hydrothermal wave properties on the intensity of laser radiation and foam density. Two sets of additional simulations were done. The first one regarded the same foams as in the previous subsections, but with the laser intensity $I = 10^{13}$ W/cm^2, one order of magnitude lower than in previous simulations (the first line of the results of Table 1). In the second set of simulations the foam density was reduced to ρ_p=5 g/cm^3.

The decreasing the laser intensity, as well as the increasing the foam density, reflect in a slow down of both homogenization process and hydrothermal wave propagation for all types of foam (large-pore, small-pore, overcritical and subcritical foams). The general reason is decreasing the temperature in a heated region. Decreasing the laser intensity of one order of magnitude at the same density leads to 4-5 times increasing of homogenization time for large-pore foam and 2-3 times increasing for small-pore foam. Hydrothermal wave speed decreases, approximately, by factor 5 in large-pore foam and by factor 3-3.5 in small-pore foam. An increase of

the foam density at the same intensity leads to an increase of the homogenization time of 1.5-2 times for both large-pore and small-pore foams. The hydrothermal wave speed decreases by, approximately, the same factors. In the large-pore foam case, the factor of decrease of the hydrothermal wave speed due to the decreasing of laser intensity is 1.5-2 times larger than for homogeneous media of the same density and this factor is, approximately, the same for small-pore foam and homogeneous media (about 2.5-3). The factor of hydrothermal wave speed decreasing due to increasing of density is, approximately, the same (1.2-1.5).

		Large-pores				Small-pores				Homogeneous	
		overcritical		subcritical		overcritical		subcritical		overcritical	subcritical
I, W/cm^2	ρ_a mg/cm^2	v_{th}, cm/s	t_h, ns	v_{th}, cm/s	t_h, ns	v_{th}, cm/s	t_h, ns	v_{th}, cm/s	t_h, ns	v_{th}, cm/s	v_{th}, cm/s
10^{13}	10	$3.6\cdot10^6$	7.6	$4.1\cdot10^6$	7.8	$4.9\cdot10^6$	0.23	$8.9\cdot10^6$	0.23	$1.4\cdot10^7$	$1.7\cdot10^7$
10^{14}	10	$1.3\cdot10^7$	1.7	$2.1\cdot10^7$	1.7	$1.8\cdot10^7$	0.09	$2.6\cdot10^7$	0.09	$3.4\cdot10^7$	$4.5\cdot10^7$
10^{13}	5	$4.8\cdot10^6$	4.0	$9.0\cdot10^6$	4.2	$1.1\cdot10^7$	0.15	$1.9\cdot10^7$	0.15	$2.2\cdot10^7$	$2.6\cdot10^7$
10^{14}	5	$2.5\cdot10^7$	1.0	$4.5\cdot10^7$	1.0	$3.1\cdot10^7$	0.06	$6.0\cdot10^7$	0.06	$5.9\cdot10^7$	$10.1\cdot10^7$

Table 1. Comparison between various foam and laser parameters for hydrothermal wave velocity and homogenization time

4. Properties of hydrothermal wave in porous substance and comparison with experiments

Numerical calculations allowed to study the complex picture of the interaction of a nanosecond laser pulse of terawatt intensity with a porous substance, taking into account the whole set of factors determining the characteristics of laser radiation absorption, hydrodynamic motion and electron thermal conductivity in the porous medium. The fundamental mechanism has been shown to be the process of plasma homogenization, whose speed depends on the characteristics of foam structure and laser intensity.

For comparison with the results of the experiments, in addition to the data of Table 1, simulations were carried out in the conditions of recent experiments on the terawatt laser beam interaction with flat porous targets, performed at Gekko-XII (Nikolai,

2012) and PALS (Khalenov, 2006; Borisenko, 2006) installations with foams of subcritical density, and at the ABC installation with foam of overcritical density. All the foams used in the Gekko-XII and PALS experiments have practically the same chemical composition, corresponding to an average atomic weight of about 7.2 and an average charge of fully ionized plasma 3.8, and also have practically the same density of solid elements about 1 $g \cdot cm^{-3}$. In these experiments, the main measurable result is the velocity of the energy transfer wave, which was determined from the temporal evolution of the image of the heated plasma with the help of X-ray streak camera, and also by recording the emission from the rear side of a foam layer of a given thickness.

The experiments performed at the Gekko-XII laser facility were done with a foam with average density of 10 mg cm^{-3} and average pore size of 1 μm. The Gekko-XII laser beam had a total energy of 300 J of 350 nm wavelength radiation (third harmonic of Nd-laser radiation) and with a 100 μm focal spot radius. The pulse down time was 3 ns. The intensity calculated from these parameters is of about $3 \cdot 10^{14}$ W/cm^2. Given the conditions of these experiments, the target can be classified in this work as a small-pore subcritical foam. The ionization wave velocity measured in these experiments is $2.9 \cdot 10^7$ cm/s. The speed of the hydrothermal wave calculated by the MULTI-FM code, is $4.9 \cdot 10^7$ cm/s. In these simulations, as well as in simulations whose results are discussed below, the average thickness of solid elements was determined on the basis of relation (1) with a fractal parameter equal to 0.8. In this case, in an equivalent homogeneous substance (with the same density), the ionization wave velocity would be $6.6 \cdot 10^7$ cm/s . The simulations with the PALE code, which, we recall, is applicable only for the modeling of subcritical foam, give a velocity of $3.6 \cdot 10^7$ cm/s. In the PALE code the characteristic temperature on the front was about 1.5 keV, in the MULTI-FM code is of 1.9 keV.

Similar experiments have been carried out at PALS laser facility. The laser pulse had a wavelength of 438 nm (third harmonic of iodine-laser radiation), a FWHM-duration of 320 ps, with a 400 μm focal spot radius and a total energy about of 170 J.

These parameters provide the intensity of about $7 \cdot 10^{14}$ W/cm^2. The experiments were carried out with the media density of 9 mg cm^{-3} and 4.9 mg cm^{-3}, and a pore size of about 1 μm, as well as in the experiments at the Gekko-XII installation. Both media are small-pore subcritical foams. The measured velocities of the ionization wave were $3.3 \cdot 10^7$ cm/s for a foam with a density of 9 mg cm^{-3} and $1.8 \cdot 10^8$ cm/s for a foam with a density of 4.9 mg cm^{-3}. In calculations using the PALE code, the speed was $5 \cdot 10^7$ cm/s and $2 \cdot 10^8$ cm / s, respectively. In the simulations with the MULTI-FM code, the speeds are $7.4 \cdot 10^7$ cm/s for a foam with a density of 9 mg cm^{-3} and $1.9 \cdot 10^8$ cm/s for a foam with a density of 4.9 mg cm^{-3}. In equivalent homogeneous media, the velocity of the ionization wave would be $9.9 \cdot 10^7$ cm/s and $2.5 \cdot 10^8$ cm/s. The difference in the results from the two codes is mainly due to the fact that MULTI-FM is a one-dimensional code, while PALE is a two-dimensional code. A two-dimensional calculation is able to reproduce also the lateral energy spread in the target, which contribute to slowing down the hydrothermal wave; this effect cannot be taken into account in a one-dimensional code. Nonetheless, in MULTI-FM simulations the hydrothermal wave speed is significantly lower in the foam than in the homogeneous medium and it is mostly quite close to the experimental number, demonstrating that the main effects of plasma homogenization are properly taken into account.

In the experiments carried out ate ABC facility at ENEA Research Center in Frascati [39], a foam target of 10 mg/cm^3 has been irradiated with the beam of Nd-laser radiation, with a 100 μm focal spot radius, total energy of 40 J and pulse duration of 3 ns. These parameters provides the intensity of about $4 \cdot 10^{13}$ W/cm^2. The diameter of the pores of the foam target was around 40 μm and solid element radius of about 1 μm. In this case, the investigated foam was a large-pore overcritical one. The measured energy transfer wave velocity was $1.5 \cdot 10^7$ cm/s. The hydrothermal wave velocity calculated by the MULTI-FM code, is $1.7 \cdot 10^7$ cm/s. In the case of equivalent homogeneous substance, the velocity of the shock wave would be $2.7 \cdot 10^7$ cm/s.

5. Conclusions

The action of terawatt laser pulse of nanosecond duration on a low-density porous substance of light chemical elements has been studied, with target densities from values less than the critical plasma density for the given laser radiation wavelength, to values exceeding the critical density. The properties of the plasma produced in these conditions have been investigated in the various regimes of pore sizes and densities by using the developed one-dimensional hydrodynamic MULTI-FM code, in which the algorithms for calculating the absorption of laser radiation, motion of matter and electron thermal conductivity take into account the peculiar internal structure of these media. The results of MULTI-FM code simulations are in a good agreement with experimental data. The experimental results together with the results of MULTI-FM code simulations confirm that the energy transfer in these materials is realized by the propagation of the hydrothermal wave, whose velocity is close to the sound velocity in the heated region of the substance. This velocity is significantly lower than the velocity of the ionization wave or the electron thermal conductivity wave, respectively, in a homogeneous substance of equivalent subcritical or overcritical density. Morevoer, the speed of hydrothermal wave increases with the growth of laser intensity and with the decrease of the initial average density. Finally, the pressure behind the front of the hydrothermal wave in the porous substance is larger, and the density, on the contrary, is less in comparison with the shock wave or the ionization wave, respectively, in a homogeneous substance of equivalent overcritical or subcritical density. The theoretical statements, confirmed by numerical simulations, explain the results of experiments on laser interaction with a foam target, including the dependence of the measured velocity of energy transfer on the laser intensity and initial density of the foam. These results are of key importance for the application of low-density foams as absorbers of laser radiation, for effectively smoothing the heterogeneities of laser energy deposition in the LTF targets. Additionally, the pressure in the laser-produced plasma in overcritical and subcritical foams is found to be larger than in an equivalent homogeneous medium. This allows

considering low-density porous media as an effective ablators, to enhance the compression of the LTF target.

Aknowledgements

This work has been carried out within the framework of the EUROfusion Consortium and has received funding from the Euratom research and training programme 2014–2018 under grant agreement No 633053. The views and opinions expressed herein do not necessarily reflect those of the European Commission.

This work was supported by the Program of Increase in the Competitiveness of the National Research Nuclear University MEPhI. The work of S. Gus'kov and A. Rupasov was also supported by Russian Foundation for Basic Research project No. 17-02-00059-a.

References

AMENDT P *et al* 2015 IFSA2015, Tu.Po.28

BATANI, D., NAZAROV, W., HALL, T., LÖWER, T., KOENIG, M., FARAL, B., BENUZZI-MOUNAIX, A., GRANDJOUAN. N., (2000). Foam-induced smoothing studied through laser-driven shock waves. *Phys. Rev. E* **62**, 8573.

BORISENKO, N. G., AKIMOVA, I. V., GROMOV, A. I., KHALENKOV, A. M., MERKULIEV, YU. A., KONDRASHOV, V. N., LIMPOUCH, J., KUBA, J., KROUSKY, E., MASEK, K., NAZAROV, W., PIMENOV, V. G. (2006). Regular 3-D Networks with Clusters for Controlled Energy Transport Studies in Laser Plasma Near Critical Density *Fusion Sci. Technol.* **49** 676

BUGROV, A. E., GUS'KOV, S. YU., ROZANOV, V. B., BURDONSKII, I. N., GAVRILOV, V. V., GOL'TSOV, A. YU., ZHUZHUKALO, E. V., KOVAL'SKII, N. G., PERGAMENT, M. I., PETRYAKOV, V. M. (1997). Interaction of a high-power laser beam with low-density porous media. *JETP*, **84**, 497.

BUGROV, A.E., BURDONSKII, I.N., GAVRILOV, V.V., GOL'TSOV, A.YU., GUS'KOV, S.YU., KOVAL'SKII, N.G., KONDRASHOV, V.N., MEDOVSHCHIKOV, S.F., PERGAMENT, M.I., PETRYAKOV, V.M., ROSANOV, V.B., ZHUZHUKALO, E.V., Investigation of light

absorption, energy transfer, and plasma dynamic processes in laser-irradiated targets of low average density. *Laser and Particle Beams*, **17**, 415.

CARUSO, A., STRANGIO, C., GUS'KOV, S.YU., ROZANOV, V.B. (2000). Interaction experiments of laser light with low density supercritical foams at the AEEF ABC facility. *Laser and Particle Beams*, **18**, 25.

CARUSO, A., GUS'KOV, S.YU., DEMCHENKO, N.N., ROZANOV, V. B., STRANGIO, C. (1997). Interaction of nanosecond laser pulses with plastic foams. *J. Russian Laser Research* **18**, 464

CIPRIANI, M. et al., in preparation.

DE ANGELIS, R., CONSOLI, F., GUS'KOV, S. YU., RUPASOV, A. A., ANDREOLI, P., CRISTOFARI, G., DI GIORGIO, G. (2015). Laser-ablated loading of solid target through foams of overcritical density. *Phys. Plasmas* **22**, 072701.

DENAVIT, J., PHILLION, D. W. (1994). Laser ionization and heating of gas targets for long‐scale‐length instability experiments. *Phys. Plasmas* **1** 1971

RAMIS, R., SCHMALTZ, R., MEYER-TER-VEHN, J. (1988). MULTI — A computer code for one-dimensional multigroup radiation hydrodynamics. *Comp. Phys. Comm.* **49** 475.

DEPIERREUX, S., LABAUNE, C., MICHEL, D. T., STENZ, C., NICOLAI, P., GRECH, M., RIAZUELO, G., WEBER, S., RICONDA, C., TIKHONCHUK, V. T., LOISEAU, P., BORISENKO, N. G., NAZAROV, W., HULLER, S., PESME, D., CASANOVA, M., LIMPOUCH, J., MEYER, C., DI-NICOLA, P., WROBEL, R., ALOZY, E., ROMARY, P., THIELL, G., SOULLIE, G., REVERDIN, C., VILLETTE, B. (2009). Laser Smoothing and Imprint Reduction with a Foam Layer in the Multikilojoule Regime. *Phys. Rev. Lett.* **102**, 195005.

DESSELBERGER, M., JONES, M. W., EDWARDS, J., DUNNE, M., WILLI, O. (1995). Use of X-Ray Preheated Foam Layers to Reduce Beam Structure Imprint in Laser-Driven Targets, *Phys. Rev. Lett.* **74**, 2961.

DUNNE, M., BORGHESI, M., IWASE, A., JONES, M. W., TAYLOR, R., WILLI, O., GIBSON, R., GOLDMAN, S. R., MACK, J., WATT, R. G. (1995). Evaluation of a Foam Buffer

Target Design for Spatially Uniform Ablation of Laser-Irradiated Plasmas. *Phys. Rev. Lett.* **75**, 3858.

FOURNIER, K. B., MAY, M. J., COLVIN, J. D., KANE, J. O., SCHNEIDER M., DEWALD, E., THOMAS, C. A., COMPTON, S., MARRS, R. E., MOODY, J., BOND, E., MICHEL, P., FISHER, J. H., NEWLANDER, C. D., DAVIS, J. F (2010). Multi-keV x-ray source development experiments on the National Ignition Facility *Phys. Plasmas* **17,** 082701.

GUS'KOV, S. YU., ZMITRENKO, N. V., ROZANOV, V. B. (1995). The "laser greenhouse" thermonuclear target with distributed absorption of laser energy. *JETP*, **81**, 296.

GUS'KOV, S. YU., ROZANOV, V. B. (1997a), Interaction of laser radiation with a porous medium and formation of a nonequilibrium plasma. *Quantum Electronics*, **27**, 696.

GUS'KOV, S.YU., CARUSO, A., ROZANOV, V.B., STRANGIO, C. (2000a). Interaction of a high-power laser pulse with supercritical-density porous materials. *Quantum Electronics*, **30**, 191.

GUS'KOV, S.YU., GROMOV, A.I., MERKUL'EV, YU.A., ROZANOV, V.B., NIKISHIN, V.V., TISHKIN, V.F., ZMITRENKO, N.V., GAVRILOV, V.V., GOL'TSOV, A.A., KONDRASHOV, V.N., KOVALSKY, N.V., PERGAMENT, M.I., GARANIN, S.G., KIRILLOV, G.A., SUKHAREV, S.A., CARUSO, A., STRANGIO, C. (2000b). Nonequilibrium laser-produced plasma of volume-structured media and ICF applications. *Laser and Particle Beams* **18**, 1.

GUS'KOV, S. YU., MERKUL'EV, YA. A. (2001). Low-density absorber—converter in direct-irradiation laser thermonuclear targets. *Quantum Electronics* **31**, 311

GUS'KOV, S. YU., DEMCHENKO, N. N., ROZANOV, V. B., STEPANOV, R. V., ZMITRENKO, N. V., CARUSO, A., STRANGIO, C. (2003). Symmetric compression of 'laser greenhouse' targets by a few laser beams. *Quantum Electronics* **33**, 95

GUS'KOV, S. YU., ZMITRENKO, N. V., ROZANOV, V. B. (1997b). Powerful thermonuclear neutron source based on laser excitation of hydrothermal dissipation in a volume-structured medium. *JETP Letters*, **66**, 555.

GUS'KOV, S. YU., CIPRIANI, M., DE ANGELIS, R., CONSOLI, F., RUPASOV, A. A., ANDREOLI, P., CRISTOFARI, G., DI GIORGIO, G. (2015). Absorption coefficient for nanosecond laser pulse in porous material. *Plasma Phys. Control. Fusion* **57** 125004

GUS'KOV, S.YU., LIMPOUCH, J., NICOLAI, PH., TIKHONCHUK, V. (2011). Laser-supported ionization wave in under-dense gases and foams. *Phys. Plasmas* **18** 103114

HALL, T., BATAN, D., NAZAROV, W., KOENIG, M. BENUZZI, A. (2002). Recent advances in laser–plasma experiments using foams. *Laser Part. Beams* **20**, 303.

KALANTAR, D., KEY, M., DASILVA, L., GLENDINNING, S., KNAUER, J., REMINGTON, B., WEBER, F. WEBER, S. (1996). Measurement of 0.35μm Laser Imprint in a Thin Si Foil Using an X-Ray Laser Backlighter. *Phys. Rev. Lett.* **76,**3574.

KAPIN, T., KUCHARIK, M., LIMPOUCH, J., LISKA, R. (2006). Hydrodynamic simulations of laser interactions with low-density foams. *Czech. J. Phys.* **56** B493–8.

KOCH, J. A., ESTABROOK, K . G., BAUER, J. D., BACK C. A. (1995). Time-resolved x-ray imaging of high power laser-irradiated underdense silica aerogels and agar foams. *Phys. Plasmas* **2**, 3820.

KHALENKOV, A.M., BORISENKO, N.G., KONDRASHOV, V.N., MERKULIEV, YU.A., LIMPOUCH, J., PIMENOV, V.G. (2006). Experience of micro-heterogeneous target fabrication to study energy transport in plasma near critical density. *Laser Part. Beams* **24** 283.

LEBO, I.G., LEBO, A. I. (2009). Interaction of high-power laser pulses with low-density targets in experiments with the PALS installation. *Matem. Mod.* **21**, 75

LIMPOUCH, J., DEMCHENKO, N. N., GUS'KOV, S. YU., KALAL, M., KASPERCZUK, A., KONDRASHOV, V. N., KROUSKÝ, E., MASEK, K., PISARCZYK, P., PISARCZYK, T., ROZANOV, V. B. (2004). Laser interactions with plastic foam—metallic foil layered targets. *Plasma Phys. Control. Fusion* **46** 1831.

NICOLAI, PH., OLAZABAL-LOUMÉ, M., FUJIOKA, S., SUNAHARA, A., BORISENKO, N., GUS'KOV, S., OREKOV, A., GRECH, M., RIAZUELO, G., LABAUNE, C., VELECHOWSKI, J., TIKHONCHUK, V. (2012). Experimental evidence of foam homogenization. *Physics of Plasmas* **19**, 113105.

NISHIMURA, H., SHIRAGA, H., AZECHI, H., MIYANAGA, N., NAKAI, M., IZUMI, N., NISHIKINO, M., HEYA, M., FUJITA, K., OCHI, Y., SHIGEMORI, K., OHNISHI, N., MURAKAMI, M., NISHIHARA, K., ISHIZAKI, R., TAKABE, H., NAGAI, K., NORIMATSU, T., NAKATSUKA, M., YAMANAKA, T., NAKAI, S., YAMANAKA, C., MIMA, K. (2000). Indirect-direct hybrid target experiments with the GEKKO XII laser. *Nucl. Fusion* **40**, 547.

PEREZ, F., PATTERSON, J. R., MAY, M., COLVIN, J. D., BIENER, M. M., WITTSTOCK, A., KUCHEYEV, S. O., CHARNVANICHBORIKARN, S., SATCHER JR., J. H., GAMMON, S. A., POCO, J. F., FUJIOKA, S., ZHANG, Z., ISHIHARA, K., TANAKA, N., IKENOUCHI, T., NISHIMURA, H., FOURNIER, K. B. (2014). Bright x-ray sources from laser irradiation of foams with high concentration of Ti. *Phys. Plasmas* **21** 023102.

V.B. ROZANOV, D.V. BARISHPOLT'SEV, G.A. VERGUNOVA et al JETP 149, 294 (2016)

VELECHOVSKY, J., LIMPOUCH, J., LISKA, R., TIKHONCHUK, V. (2016), Hydrodynamic modeling of laser interaction with micro-structured targets. *Plasma Phys. Control. Fusion* **58** 095004.

WATT, R. G., WILSON, D. C., CHRIEN, R. E., HOLLIS, R. V., GOBBY, P. L., MASON, R. J., KOPP, R. A. (1997). Foam-buffered spherical implosions at 527 nm. *Phys. Plasmas* **4**, 1379.

WATT, R. G., DUKE, J., FONTES, C. J., GOBBY, P. L., HOLLIS, R. V., KOPP, R. A., MASON, R. J., WILSON, D. C., VERDON, C. P., BOEHLY, T. R., KNAUER, J. P., MEYERHOFER, D. D., SMALYUK, V., TOWN, R. P. J., IWASE, A., WILLI O. (1998). Laser Imprint Reduction Using a Low-Density Foam Buffer as a Thermal Smoothing Layer at 351-nm Wavelength. *Phys. Rev. Lett.* **81**, 4644.